

Supporting Information

Manganese(II) enhanced fluorescent nitrogen-doped graphene quantum dots: a facile and efficient synthesis and their applications for bioimaging and detection of Hg²⁺ ions

¹Li Yang, ¹Aimiao Qin*, ¹Shuoping Chen, ¹Lei Liao, ²Jiangke Qin,
¹Kaiyou Zhang

¹Key Lab New Processing Technology for Nonferrous Metals & Materials Ministry of
Education, Guangxi Key Laboratory in Universities of Clean Metallurgy and
Comprehensive Utilization for Non-ferrous Metals Resources, College of Materials
Science & Engineering, Guilin University of Technology, Guilin, China

²College of Chemistry and Pharmaceutical Science, Guangxi Normal university,
Guilin, China

This supporting information includes:

Quantum yield measurements, the concentrations of Mn(II)-NGQDs solution test,
Cellular toxicity test, Fluorescence life time, Table S1, Table S2, Table S3, Fig. S1,
Fig. S2, Fig. S3(a)-(b), Fig. S4, Fig. S5(a)-(d), Fig. S6(a)-(f), Fig.S7(a)-(f), Fig. S8,
Fig. S9.

Quantum yield measurements

The quantum yield (QY) of the Mn(II)-NGQDs, NG and M-NG were determined according to an established procedure using quinine sulfate (with QY of 54%, 0.1 M H₂SO₄ as a solvent) as a reference. In order to minimize the reabsorption effects, absorbencies in the 10 mm fluorescence cuvette were kept between 0.02 to 0.05 at the excitation wavelength (360 nm) [S1]. The QY of the QDs was calculated according to the below equation:

$$\varphi_x = \varphi_{re} \times (I_x/I_{re}) \times (A_{re}/A_x) \times (n_x/n_{re})^2$$

Where φ is the QY, I is the measured integrated emission intensity, A is the absorbance and n is the refractive index of the solvent. The subscript “x” refers to the sample and “re” refers to the reference with known QY. For these solutions, $n_x = n_{re} = 1.33$.

The concentrations of Mn(II)-NGQDs solution test

The calculation method of the concentrations of Mn(II)-NGQDs solution was described as follow: After the hydrothermal reaction finished, the obtained bright transparent solution was centrifuged at 10000 rpm/min for 10 min to remove the deposit. Subsequently, the supernatant of Mn(II)-NGQDs solution (V mL) was added to glass bottle. Afterwards, the pure solid-state Mn(II)-NGQDs white powder was obtained by vacuum freeze drying, and the quality was recorded (named M). Besides, the quality of empty bottle was also recorded (named M_0). Finally, the calculated concentration of Mn(II)-NGQDs solution was 6.52 mg/mL, and this concentration value was used as a standard for further application of Hg²⁺ ions detection, MTT test

and cell fluorescence imaging.

$$\text{Concentrations of Mn(II)-NGQDs (mg/mL)} = (M - M_0)/V$$

Cellular toxicity test

The cytotoxicity of Mn(II)-NGQDs was evaluated by using the MTT assay^[S2]. HepG2 human liver cancer cells were harvested (the cell density was adjusted to 10^5 cells per mL) and seeded in a 96-well plate overnight for 24 h. Then, the Mn(II)-NGQDs solution was added into each well with increasing concentrations from 0 to 300 $\mu\text{g/mL}$. After that, the cells were cultivated for 4 and 24 h, respectively. And then, 10 μL of 5 mg/mL MTT (3 - (4,5 -dimethylthiazol -2-yl) -2,5 -diphenyltetra -zolium bromide) solution were added to each cell well. After incubation for 4 h, the culture medium was discarded, and 100 μL of dimethyl sulfoxide (DMSO) was added. The obtained mixture was shaken for 15 min in the dark at room temperature, and the absorbance of each well was measured at wavelength of 570 nm using an enzyme linked immunosorbent assay (Tecan Infinite M1000) reader with pure DMSO as a blank. In addition, HepG2 human liver cancer cells without Mn(II)-NGQDs treating were used as a control to test their relative cell viability. The cell viability was calculated according to the following equation:

$$\text{Cell viability (\%)} = \left(\frac{OD_{treated}}{OD_{control}} \right) \times 100\%$$

(where $OD_{treated}$ was obtained in the presence of Mn(II)-NGQDs, and $OD_{control}$ was obtained in the absence of Mn(II)-NGQDs.)

Fluorescence life time test

Fluorescence life time was determined using time correlated single photon counting technique^[S3]. The emission decay curves of Mn(II)-NGQDs and NG in different solutions are shown in Fig.S8. Decays were recorded for Mn(II)-NGQDs and NG with emission and excitation wavelengths at 440 nm and 369.6 nm respectively.

Decay curves were fitted using multi exponential model as the following Eq1:

$$R(t)=B_1e^{(-t/\tau_1)}+ B_2e^{(-t/\tau_2)}+ B_3e^{(-t/\tau_3)} \quad (1)$$

where $R(t)$ is the intensity usually as summed to decay as the sum of individual single exponential decays, B_1 , B_2 and B_3 are the pre-exponential factors, τ_1 , τ_2 and τ_3 are the decay times. The average life time (τ_{ave}) of Mn(II)-NGQDs in the presence of different concentration of Hg^{2+} in HMTA (pH=7.35) solution was determined by Eq2.

$$\tau_{ave} = \Sigma_i B_i \tau_i^2 / \Sigma_i B_i \tau_i \quad (2)$$

Table S1 The peaks table of Mn(II)-NGQDs and NG.

Elements Sample	C1s atomic%	N1s atomic%	O1s atomic%	Mn2p atomic%
NG	60.48	2.2	37.33	0
Mn(II)-NGQDs	55.43	4.24	40.11	0.21

Table S2 Comparison of different fluorescent probs for Hg²⁺ detection.

Fluorescence probe	QY (%)	LOD (mol/L)	Linear range (mol/L)	Ref.
Valine-functionalized GQDs	28.07	0.4×10^{-8}	$0.8 \times 10^{-8} - 1 \times 10^{-6}$	46
WS ₂ nanosheet	—	3.3×10^{-8}	$6 \times 10^{-8} - 4.5 \times 10^{-6}$	47
Nitrogen-rich quantum dots(N-dots)	7.6	0.63×10^{-6}	$0 - 20 \times 10^{-6}$	48
Nitrogen-doped carbon quantum dots (N-CQDs)	15.7	0.23×10^{-6}	$0 - 3 \times 10^{-5}$	49
Carbon dots	82.40	0.234×10^{-6}	$0 - 2.5 \times 10^{-5}$	50
Mn(II)-NGQDs	42.16	3.4×10^{-8}	$0 - 3.5 \times 10^{-6}$	This work

Table S3 Fluorescence decay time (τ_{ave}) and pre-exponential factor (B) of Mn(II)-NGQDs and NG

sample	τ_1 (ns)	τ_2 (ns)	τ_3 (ns)	B_1	B_2	B_3	χ^2	τ_{ave} (ns)
NG	1.25	5.45	11.96	4359.10	3384.9 3	2866.47	1.046	8.88
Mn(II)-NGQDs	7.58	—	—	10297.64	—	—	1.084	7.58
Mn(II)-NGQDs+HMTA	7.50	—	—	10161.58	—	—	1.274	7.50
Mn(II)-NGQDs+HMTA + 2.0×10^{-6} mol/L Hg^{2+}	7.44	—	—	9897.96	—	—	1.244	7.44
Mn(II)-NGQDs+HMTA + 4.0×10^{-6} mol/L Hg^{2+}	7.41	—	—	10492.08	—	—	1.217	7.41

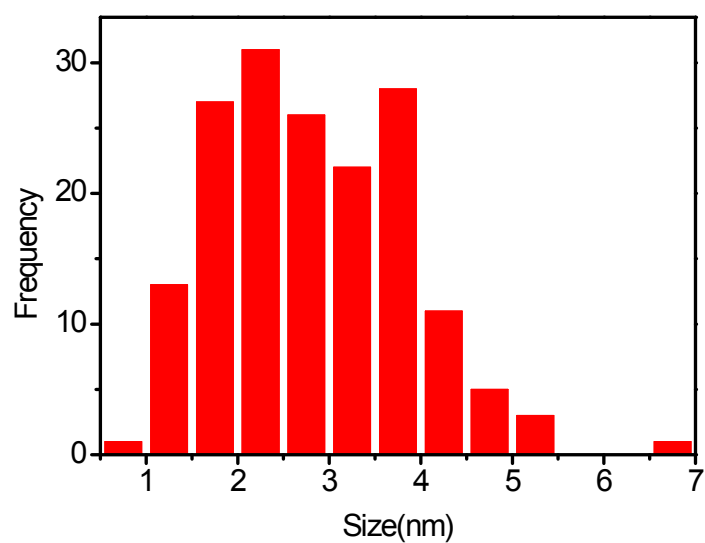


Fig. S1 Size distribution of the as-synthesized Mn(II)-NGQDs

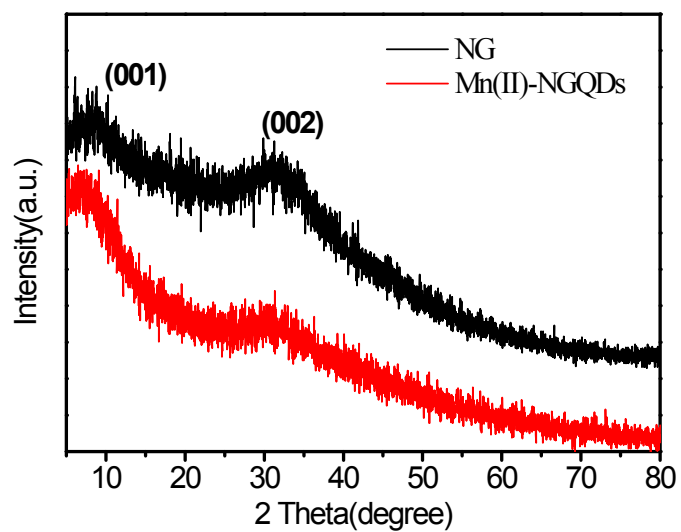


Fig. S2 XRD patterns of the Mn(II)-NGQDs and NG.

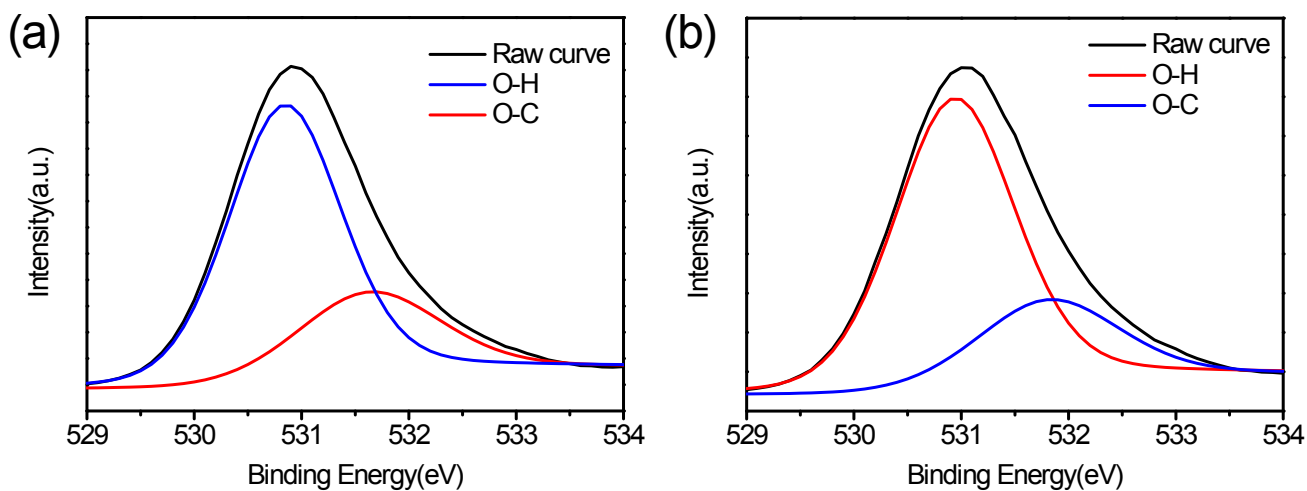


Fig. S3 The O1s spectra of Mn(II)-NGQDs (a) and NG (b).

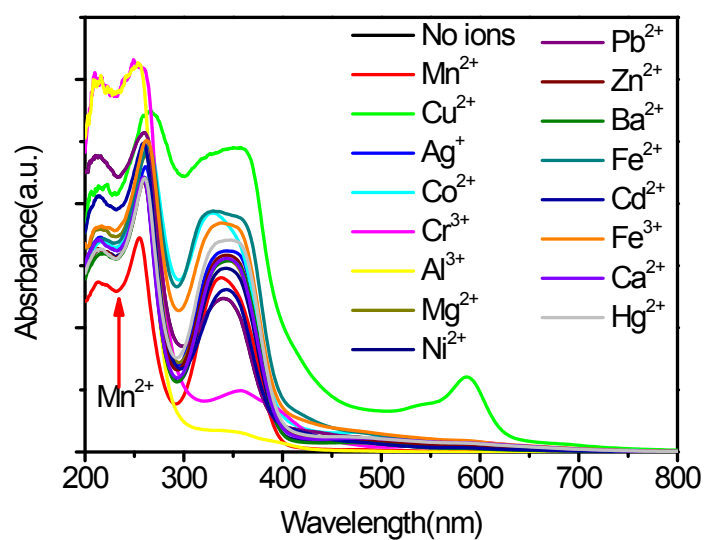


Fig. S4 The UV-vis absorption spectra of Mn(II)-NGQDs, M-NG and NG.

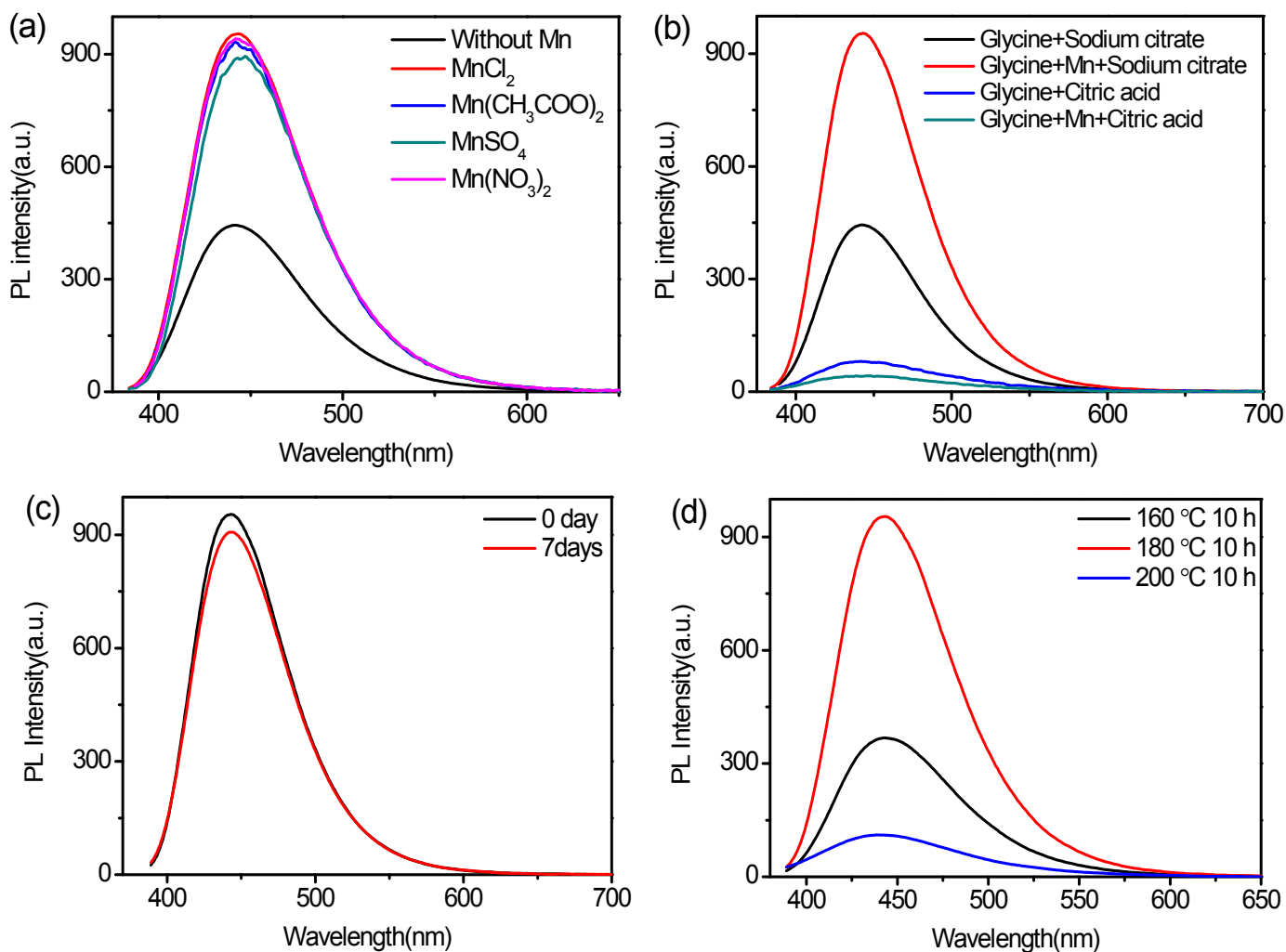


Fig. S5 (a) The PL spectra of Mn(II)-NGQDs prepared at different manganese(II) source with the 370 nm excitation wavelength; (b) The PL spectra of Mn(II)-NGQDs and NG prepared at different precursor; (c) The PL spectra of Mn(II)-NGQDs kept for 0 and 7 days at ambient temperature; (d) The emission spectra of Mn(II)-NGQDs prepared at different temperatures with the 370 nm excitation wavelength.

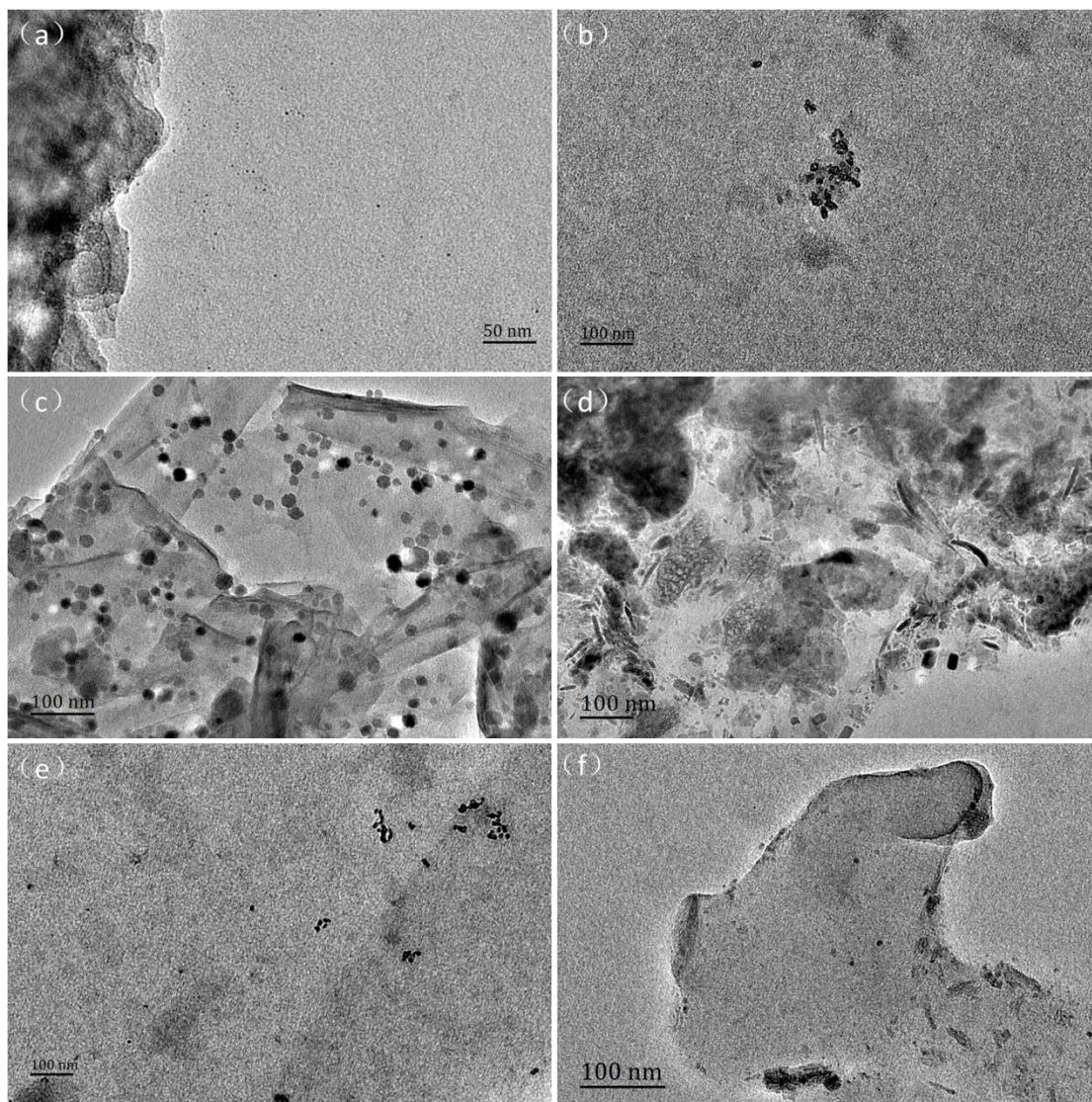


Fig. S6 TEM images of M-NG doped with different metal ions (a) Ag^+ , (b) Ni^{2+} , (c) Fe^{2+} , (d) Co^{2+} , (e) Mg^{2+} , (f) Zn^{2+} .

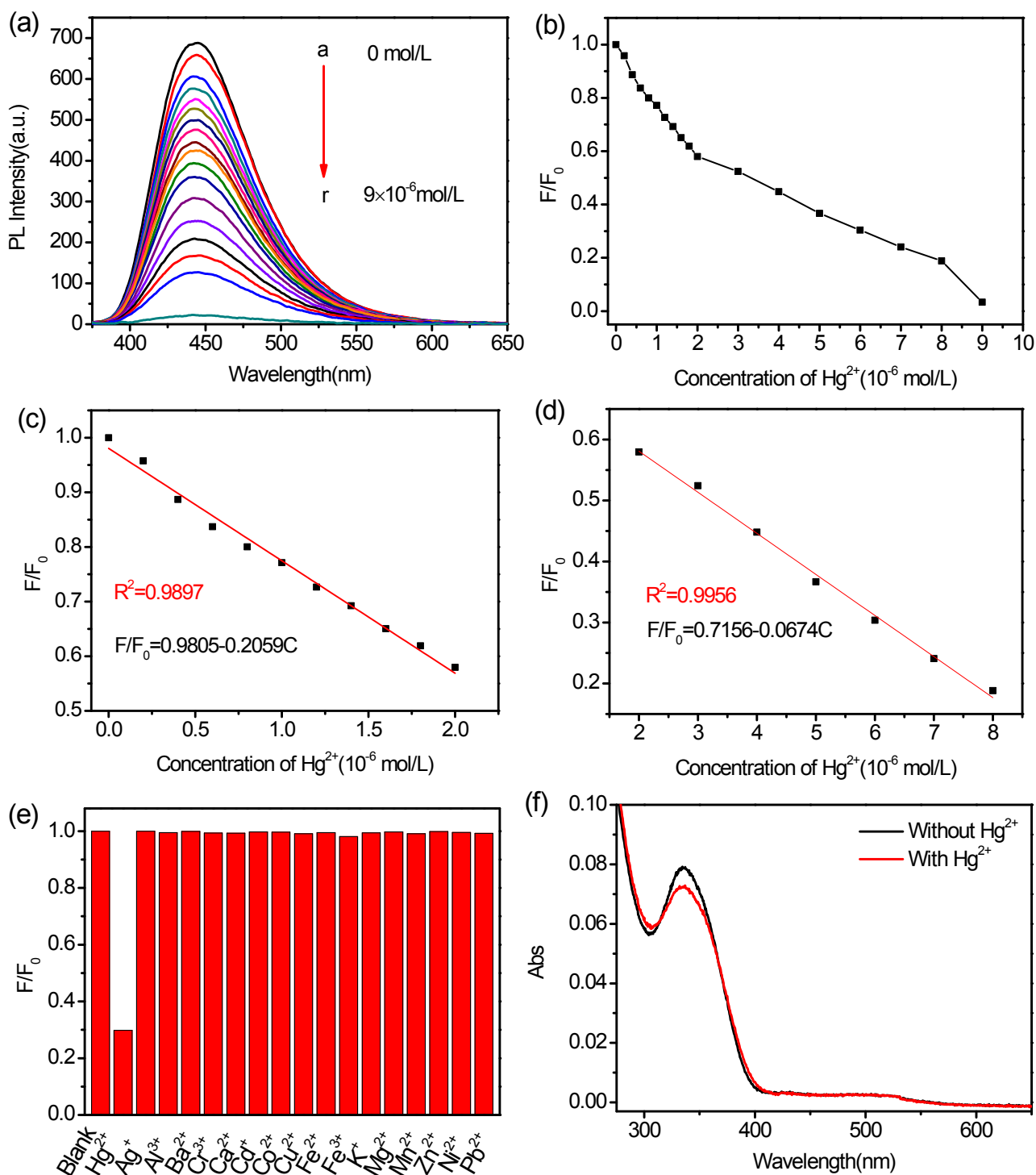


Fig. S7 (a) Emission spectra ($\lambda_{\text{ex}} = 370 \text{ nm}$) of Mn(II)-NGQDs in the presence of different concentrations of Hg²⁺ (from 0 to 9 × 10⁻⁶ mol/L) in Milli-Q water. a: 0 × 10⁻⁶ mol/L, b: 0.2 × 10⁻⁶ mol/L, c: 0.4 × 10⁻⁶ mol/L, d: 0.6 × 10⁻⁶ mol/L, e: 0.8 × 10⁻⁶ mol/L, f: 1.0 × 10⁻⁶ mol/L, g: 1.2 × 10⁻⁶ mol/L, h: 1.4 × 10⁻⁶ mol/L, i: 1.6 × 10⁻⁶ mol/L, j: 1.8 × 10⁻⁶

mol/L, k: 2.0×10^{-6} mol/L, l: 3.0×10^{-6} mol/L, m: 4.0×10^{-6} mol/L, n: 5.0×10^{-6} mol/L, o: 6.0×10^{-6} mol/L, p: 7.0×10^{-6} mol/L, q: 8.0×10^{-6} mol/L, r: 9.0×10^{-6} mol/L; (b) The relationship between the F/F_0 and Hg^{2+} concentrations (c: $0-9.0 \times 10^{-6}$ mol/L); (c) Plots of intensity ratio of F/F_0 versus the concentrations of Hg^{2+} ($0-2.0 \times 10^{-6}$ mol/L); (d) Plots of intensity ratio of F/F_0 versus the concentrations of Hg^{2+} ($2.0 \times 10^{-6}-8.0 \times 10^{-6}$ mol/L); (e) Fluorescence responses of Mn(II)-NGQDs to the different metal ions in Milli-Q water. The concentration of each metal ion is 6.0×10^{-6} mol/L. F_0 and F correspond to the fluorescence intensities of Mn(II)-NGQDs at 440 nm with the 370 nm excitation wavelength in the absence and presence of metal ions, respectively; (f) The UV absorption spectra of Mn(II)-NGQDs without Hg^{2+} and in the presence of Hg^{2+} (6.0×10^{-6} mol/L).

The linear relationship of F/F_0 versus Hg^{2+} ions concentration is in the range of 0 mol/L to 2.0×10^{-6} mol/L (Fig. S7c,) and 2.0×10^{-6} mol/L to 8.0×10^{-6} mol/L (Fig. S7d), and the detection limit of 3.2×10^{-7} mol/L.

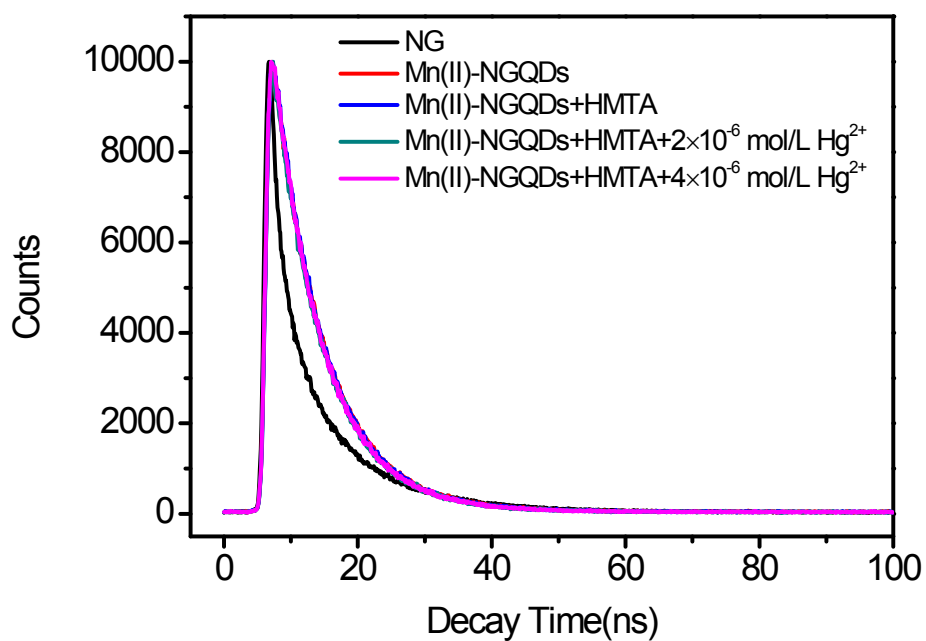


Fig. S8 Fluorescence decay curves of Mn(II)-NGQDs in the presence of different concentration of Hg^{2+} in HMTA buffer solution (pH=7.35) with emission monitored at 440nm and excitation at 369.6 nm.

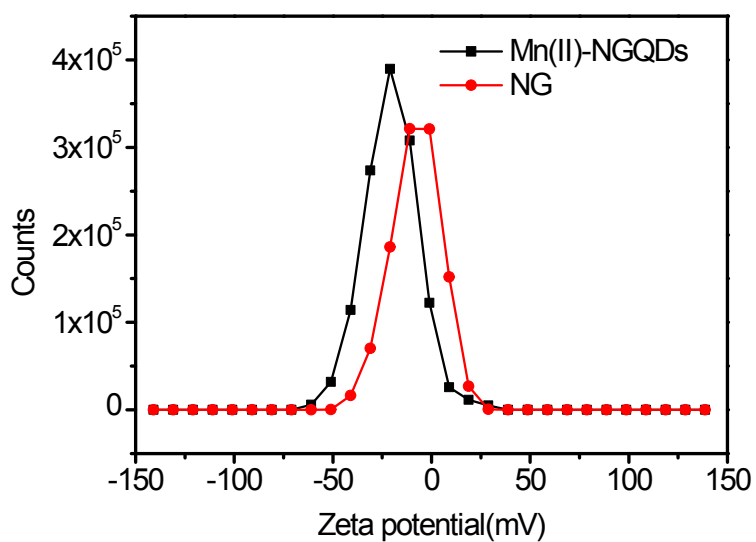


Fig. S9 Zeta potential of Mn(II)-NGQDs and NG

References

- [S1] J. Liao, Z. Cheng and L. Zhou, *ACS Sustain. Chem. & Eng.*, 2016, **4**, 3053-3061.
- [S2] S. Y. Choi, S. H. Baek, S. J. Chang, Y. Song, R. Rafique, K. T. Lee and T. J. Park, *Biosens. Bioelectron.*, 2017, **93**, 267-273.
- [S3] Y. Zhang, P. Cui, F. Zhang, X. Feng, Y. Wang, Y. Yang and X. Liu, *Talanta*, 2016, **152**, 288-300.